AMERICAN SOCIETY FOR MICROBIOLOGY | Journal of Bacteriology®

RESEARCH ARTICLE

Three Distinct Contact-Dependent Growth Inhibition Systems Mediate Interbacterial Competition by the Cystic Fibrosis Pathogen *Burkholderia dolosa*

Andrew I. Perault,[a] Peggy A. Cotter[a]

[a]Department of Microbiology and Immunology, University of North Carolina at Chapel Hill, Chapel Hill, North Carolina, USA

ABSTRACT The respiratory tracts of individuals afflicted with cystic fibrosis (CF) harbor complex polymicrobial communities. By an unknown mechanism, species of the Gram-negative *Burkholderia cepacia* complex, such as *Burkholderia dolosa*, can displace other bacteria in the CF lung, causing cepacia syndrome, which has a poor prognosis. The genome of *B. dolosa* strain AU0158 (*Bd*AU0158) contains three loci that are predicted to encode contact-dependent growth inhibition (CDI) systems. CDI systems function by translocating the toxic C terminus of a large exoprotein directly into target cells, resulting in growth inhibition or death unless the target cells produce a cognate immunity protein. We demonstrate here that each of the three *bcpAIOB* loci in *Bd*AU0158 encodes a distinct CDI system that mediates interbacterial competition in an allele-specific manner. While only two of the three *bcpAIOB* loci were expressed under the *in vitro* conditions tested, the third conferred immunity under these conditions due to the presence of an internal promoter driving expression of the *bcpI* gene. One *Bd*AU0158 *bcpAIOB* allele is highly similar to *bcpAIOB* in *Burkholderia thailandensis* strain E264 (*Bt*E264), and we showed that their BcpI proteins are functionally interchangeable, but contact-dependent signaling (CDS) phenotypes were not observed in *Bd*AU0158. Our findings suggest that the CDI systems of *Bd*AU0158 may provide this pathogen an ecological advantage during polymicrobial infections of the CF respiratory tract.

IMPORTANCE Human-associated polymicrobial communities can promote health and disease, and interbacterial interactions influence the microbial ecology of such communities. Polymicrobial infections of the cystic fibrosis respiratory tract impair lung function and lead to the death of individuals suffering from this disorder; therefore, a greater understanding of these microbial communities is necessary for improving treatment strategies. Bacteria utilize contact-dependent growth inhibition systems to kill neighboring competitors and maintain their niche within multicellular communities. Several cystic fibrosis pathogens have the potential to gain an ecological advantage during infection via contact-dependent growth inhibition systems, including *Burkholderia dolosa*. Our research is significant, as it has identified three functional contact-dependent growth inhibition systems in *B. dolosa* that may provide this pathogen a competitive advantage during polymicrobial infections.

KEYWORDS Bcc, *Burkholderia*, contact-dependent inhibition, interbacterial competition, two-partner secretion

Bacteria often reside in complex polymicrobial communities in which intra- and interspecies interactions influence community structure (1–4), and interbacterial competition has been proposed to have a greater impact on microbial ecology and evolution within polymicrobial environments than interbacterial cooperation (5). While complex microbial communities, such as the microbiota of the intestinal and vaginal

Received 16 July 2018 **Accepted** 23 August 2018

Accepted manuscript posted online 27 August 2018

Citation Perault AI, Cotter PA. 2018. Three distinct contact-dependent growth inhibition systems mediate interbacterial competition by the cystic fibrosis pathogen *Burkholderia dolosa*. J Bacteriol 200:e00428-18. https://doi.org/10.1128/JB.00428-18.

Editor Victor J. DiRita, Michigan State University

Copyright © 2018 American Society for Microbiology. All Rights Reserved.

Address correspondence to Peggy A. Cotter, peggy_cotter@med.unc.edu.

tracts, can promote the health of their hosts (6, 7), microbial communities can also arise in diseased tissues and exacerbate morbidity, such as in the respiratory tracts of cystic fibrosis (CF) patients. Several bacterial pathogens, including *Staphylococcus aureus*, *Pseudomonas aeruginosa*, and members of the *Burkholderia cepacia* complex (Bcc), are notorious for dominating the CF airways, (8, 9). Infections by Bcc pathogens typically do not arise until teenage years or adulthood and can rapidly progress to "cepacia syndrome," which is a fatal, necrotizing pneumonia accompanied by bacteremia (10, 11). Strikingly, Bcc pathogens can replace other pathogenic species as the predominant organisms during polymicrobial infections, though the mechanisms underlying this behavior remain unknown (12–14).

Contact-dependent growth inhibition (CDI) is a mechanism of interbacterial competition in which the toxic C terminus (CT) of a large exoprotein belonging to the two-partner secretion (TPS) family is delivered directly from one bacterium to another, resulting in death or growth arrest of the recipient cell (15). Autotoxicity is prevented in CDI^+ cells by the production of an immunity protein that binds to the CT, blocking its activity (15). Genes encoding CDI systems are widespread among Gram-negative bacteria and are polymorphic in nature, with different alleles encoding unique CT toxins and cognate immunity proteins, and thus protection against toxicity by immunity proteins occurs in an allele-specific manner (16).

Two classes of CDI systems have been described to date: the *Burkholderia* type and the *Escherichia coli* type (15–17). *E. coli*-type systems are encoded by *cdiBAI* genes, with *cdiA* encoding the toxic exoprotein, *cdiB* encoding its TPS transporter partner protein, and *cdiI* encoding the immunity protein (15). *Burkholderia*-type systems are encoded by *bcpAIOB* genes (17). *bcpA* and *bcpB* encode the exoprotein and transporter TPS proteins, respectively, *bcpI* encodes the immunity protein, and a fourth open reading frame (ORF), *bcpO*, encodes a small protein of unknown function (17). In both *E. coli*- and *Burkholderia*-type CDI systems, the N-terminal ~2,800 amino acids (aa) of CdiA and BcpA proteins, respectively, are conserved among closely related species, while the C-terminal ~300 amino acids vary greatly, as do the CdiI and BcpI proteins, allowing for toxin-antitoxin heterogeneity across different CDI system-encoding alleles (16, 18). *Burkholderia*- and *E. coli*-type CDI systems also contain distinct motifs separating the conserved and variable domains of the toxic exoproteins; NX(E/Q)LYN in BcpA proteins and VENN in CdiA proteins (16, 17). *Burkholderia*-type CDI systems are further classified into two different phylogenetic groups—class I and class II—based on the amino acid sequences of the BcpB and BcpO proteins and the conserved region of BcpA (17, 19). BcpO proteins across different *Burkholderia* class I alleles are nearly identical, save for the N-terminal ~20-aa-long signal sequence that covaries with BcpA-CT and BcpI, whereas the *bcpO* genes of class II are not similar across different alleles (17, 19).

Most information available for *Burkholderia*-type CDI systems is for the class I allele in *B. thailandensis* strain E264 (*Bt*E264) (17, 19–21). We and others have shown that the *Bt*E264 BcpAIOB proteins compose a functional CDI system (17) and that chimeric *Bt*E264 strains producing the BcpA-CTs and BcpI proteins of pathogenic *B. pseudomallei* strains outcompete neighboring cells in a CDI-dependent manner (19, 22, 23). Our laboratory has also discovered that the *Bt*E264 CDI system induces gene expression changes that promote cooperative behaviors between kin cells (i.e., cells that contain identical Bcp alleles) (24), a phenomenon we call "contact-dependent signaling" (CDS). We hypothesize that delivery of the BcpA-CT to a neighboring kin cell and subsequent BcpA-CT-BcpI binding forms a signaling complex that leads to expression of genes that confer community behaviors, including autoaggregation, biofilm formation, and pigment production (18, 21, 24).

Burkholderia dolosa, a member of the Bcc that caused a deadly epidemic in CF patients in Boston during the 1990s (25, 26), can transmit from human to human and lead to significant decline in lung function compared to uninfected CF patients (27, 28). The genome of *B. dolosa* strain AU0158 (*Bd*AU0158) contains three *bcpAIOB* loci, each potentially encoding a CDI system; one class I allele and two class II alleles. The goal of

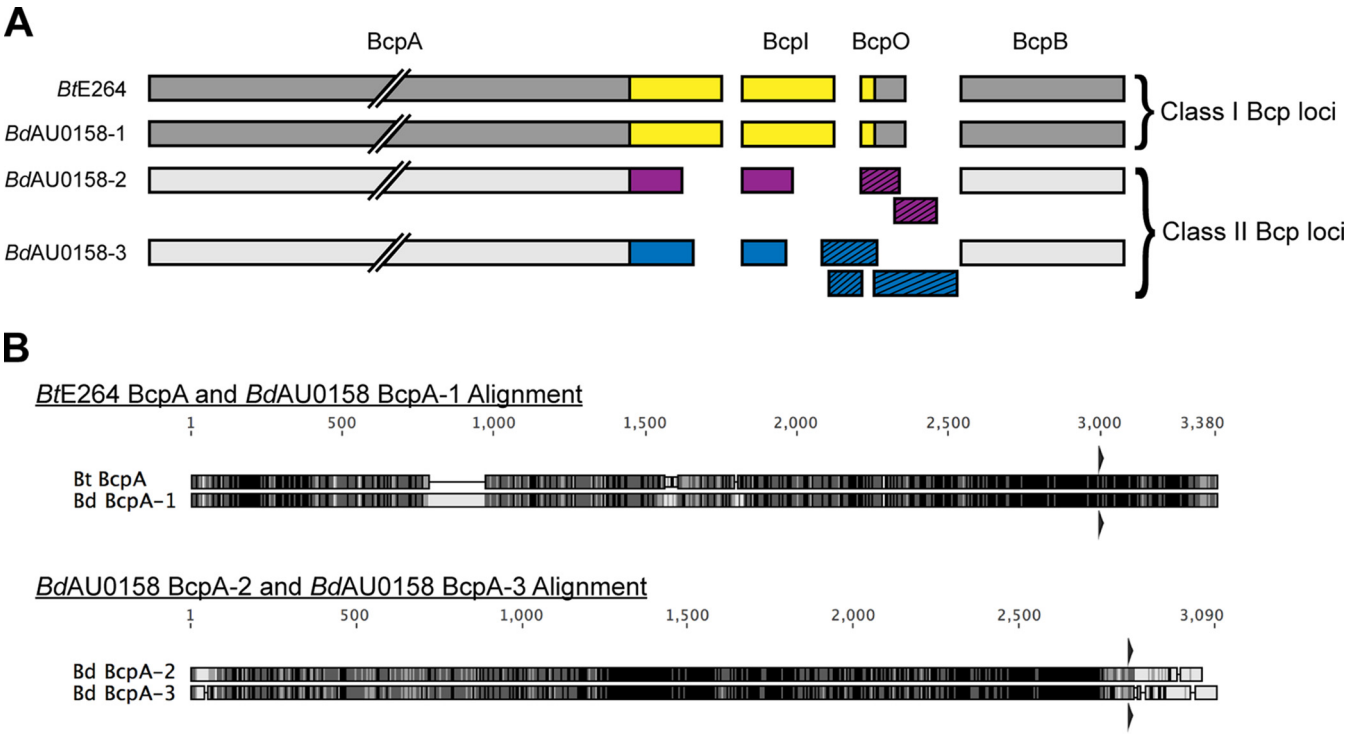

FIG 1 *bcpAIOB* loci in *Bd*AU0158. (A) Schematic of the BcpAIOB proteins encoded by the *Bd*AU0158 *bcp-1* (*Bd*AU0158-1), *bcp-2* (*Bd*AU0158 *bcp-2*), and *bcp-3* (*Bd*AU0158-3) loci, as well as the BcpAIOB proteins encoded by the *Bt*E264 *bcp* locus. Gray coloration corresponds to conserved regions of the proteins, whereas variable regions spanning BcpA-CT, BcpI, and BcpO are denoted in yellow (for the *Bt*E264 and *Bd*AU0158-1 alleles), purple (for the *Bd*AU0158-2 allele), and blue (for the *Bd*AU0158-3 allele). Potential BcpO proteins encoded by the *Bd*AU0158 *bcp-2* and *bcp-3* loci are indicated by slashed boxes. (B) Amino acid alignments of *Bt*E264 BcpA and *Bd*AU0158 BcpA-1 and of *Bd*AU0158 BcpA-2 and *Bd*AU0158 BcpA-3. Residue similarity is denoted by grayscale, with black indicating identical residues and white indicating disparate residues. Triangles above and below alignments represent NX(E/Q)LYN motifs.

this study was to characterize the *bcpAIOB* loci and potential CDI systems of *Bd*AU0158 using the native pathogenic strain.

RESULTS

The *Burkholderia dolosa* AU0158 (*Bd*AU0158) genome contains three *bcpAIOB* alleles. By searching for homologs of the *Bt*E264 *bcpB* gene, we previously detected two *bcpAIOB* alleles in *Bd*AU0158 (17). Further investigation revealed a third *bcpAIOB* locus in *Bd*AU0158. All three loci resemble *Burkholderia*-type CDI system-encoding genes, with the gene order being *bcpAIOB* and the presence of a fourth ORF, *bcpO*, between *bcpI* and *bcpB*. We will refer to these *bcpAIOB* loci as *bcp-1* (locus tags AK34_RS22045 to AK34_RS22035, chromosome 1), *bcp-2* (locus tags AK34_RS06120 to AK34_RS06110, chromosome 2), and *bcp-3* (locus tags AK34_RS04315 to AK34_RS04310, chromosome 2) (Fig. 1A). The *Bd*AU0158 *bcp-1* allele belongs to the class I family of *bcpAIOB* alleles, whereas the *Bd*AU0158 *bcp-2* and *Bd*AU0158 *bcp-3* alleles belong to the class II family. Accordingly, the BcpA proteins encoded by the *bcp-2* allele (BcpA-2) and the *bcp-3* allele (BcpA-3) are more similar to one another than they are to the BcpA protein encoded by the *bcp-1* allele (BcpA-1) (Fig. 1A). Strikingly, the *Bd*AU0158 *bcp-1* allele is highly similar to the *bcp* allele of *Bt*E264 (Fig. 1B), which we previously determined encodes a CDI system in *Bt*E264 (17). The *Bd*AU0158 BcpA-1 and the *Bt*E264 BcpA proteins share 83.0% amino acid identity overall, with 86.4% amino acid identity at the C termini (CTs). In contrast, the *Bd*AU0158 BcpA-2 and BcpA-3 proteins share 79.7% identity overall, with only 19.9% similarity between their CTs (Fig. 1B). Phyre2 analysis (29) predicts all three *Bd*AU0158 BcpA-CTs to be nucleases. All three *Bd*AU0158 *bcp* loci contain potential *bcpO* genes, with the gene of the *bcp-1* locus (*bcpO-1*) being nearly identical to *Bt*E264 *bcpO* (*Bd*AU0158 BcpO-1 and *Bt*E264 BcpO share 94.4% identity at the amino acid level after removal of the signal sequence). ORF prediction

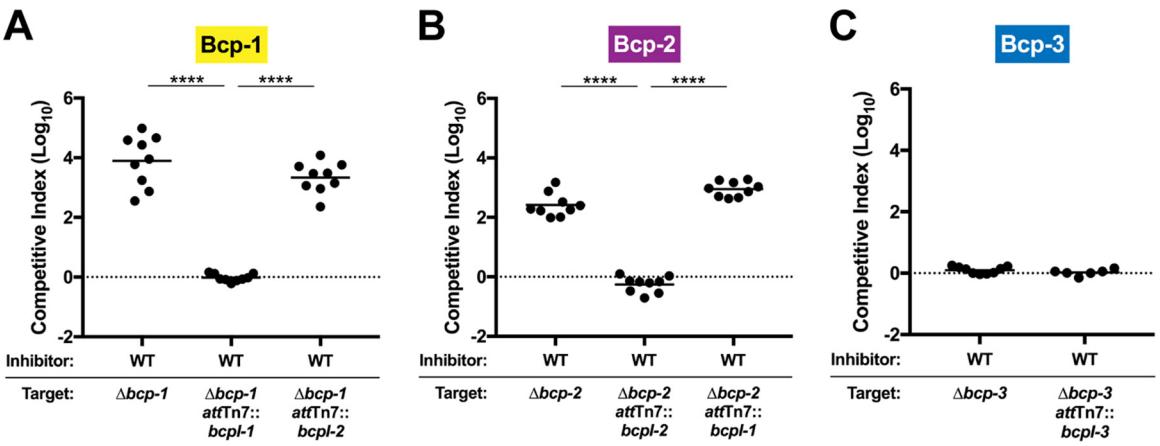

FIG 2 The Bcp-1 and Bcp-2 CDI systems provide *Bd*AU0158 a competitive advantage during *in vitro* growth. (A) Competition assays between *Bd*AU0158 WT inhibitor cells and Δ*bcp-1*, Δ*bcp-1* *att*Tn*7*::*bcpI-1*, and Δ*bcp-1* *att*Tn*7*::*bcpI-2* target cells. (B) Competition assays between *Bd*AU0158 WT inhibitor cells and Δ*bcp-2*, Δ*bcp-2* *att*Tn*7*::*bcpI-2*, and Δ*bcp-2* *att*Tn*7*::*bcpI-1* target cells. (C) Competition assays between *Bd*AU0158 WT inhibitor cells and Δ*bcp-3* and Δ*bcp-3* *att*Tn*7*::*bcpI-3* target cells. For each competition, results from three separate biological replicates, each with three technical replicates (except for the WT versus Δ*bcp-3* *att*Tn*7*::*bcpI-3* competitions in panel C, which show two biological replicates, each with three technical replicates). Solid horizontal lines represent mean $\log_{10}$ C.I. values. The dotted lines ($\log_{10}$ C.I. = 0) indicate no competitive advantage for inhibitor or target strain. ****, $P < 0.0001$, Mann-Whitney test.

software (30) detects two potential ORFs in the intergenic region between *bcpI-2* and *bcpB-2* and three potential ORFs in the intergenic region between *bcpI-3* and *bcpB-3* (Fig. 1A).

The *Bd*AU0158 *bcp-1* and *bcp-2* loci encode functional CDI systems. To determine if the *bcp* loci of *Bd*AU0158 encode functional CDI systems, mutant strains containing unmarked, in-frame deletions lacking all but the first three codons of *bcpA* and the last three codons of *bcpB* in each of the *bcp* loci were generated (Δ*bcp-1*, Δ*bcp-2*, and Δ*bcp-3*), and these mutants were competed against wild-type (WT) *Bd*AU0158. All competitions were conducted on low-salt LB (LSLB; NaCl concentration, 5 g/liter) agar for 48 h at 37°C with 1:1 initial inhibitor/target ratios. WT *Bd*AU0158 outcompeted the Δ*bcp-1* mutant by approximately 4 log (Fig. 2A) and outcompeted the Δ*bcp-2* mutant by approximately 2.5 log (Fig. 2B). To determine if the competitive exclusion in favor of WT *Bd*AU0158 was CDI dependent, the Δ*bcp-1* and Δ*bcp-2* mutants were complemented at the *att*Tn*7* site with either cognate *bcpI* genes (*bcpI-1* for the Δ*bcp-1* mutant, *bcpI-2* for the Δ*bcp-2* mutant) or heterologous *bcpI* genes (*bcpI-2* for the Δ*bcp-1* mutant, *bcpI-1* for the Δ*bcp-2* mutant), with all *bcpI* genes present in *trans* under the control of the constitutive promoter of the *Bt*E264 ribosomal S12 subunit gene (P_{S12}). The Δ*bcp-1* mutant was rescued from killing by WT *Bd*AU0158 ($\log_{10}$ competitive index [C.I.] $\approx$ 0) only when provided the cognate *bcpI-1* gene in *trans* (Fig. 2A), and the Δ*bcp-2* mutant was rescued from killing by WT *Bd*AU0158 only when provided its cognate *bcpI-2* gene in *trans* (Fig. 2B). We did not observe growth rate differences between WT *Bd*AU0158 and the Δ*bcp* mutants during *in vitro* growth, and the lack of competition between WT inhibitor strains and target mutant strains complemented with cognate *bcpI* genes suggests that the ability of WT *Bd*AU0158 to outcompete the Δ*bcp-1* and Δ*bcp-2* strains is solely due to CDI. These data indicate that the *Bd*AU0158 *bcp-1* and *bcp-2* loci encode functional CDI systems that can kill or inhibit the growth of neighboring cells lacking cognate BcpI proteins.

Unlike the *Bd*AU0158 Δ*bcp-1* and Δ*bcp-2* mutant strains, the Δ*bcp-3* mutant was not outcompeted by WT during 48 h of coculture on solid medium (Fig. 2C). Two possible explanations for this finding are that the *bcp-3* locus does not encode a functional CDI system and that the *bcp-3* locus is not expressed under the *in vitro* competition conditions used.

Unlike the *Bd*AU0158 *bcp-1* and *bcp-2* loci, the *bcp-3* locus is not expressed under *in vitro* competition conditions. To investigate expression of the *Bd*AU0158

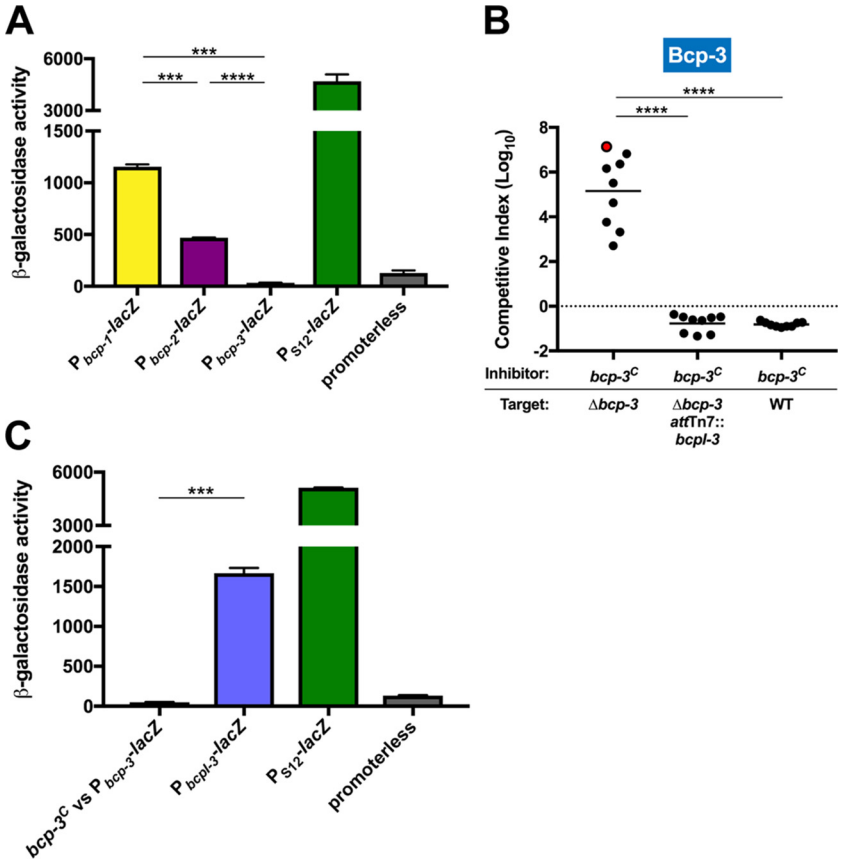

FIG 3 The *Bd*AU0158 *bcp-3* locus encodes a functional CDI system that is not expressed under *in vitro* competition conditions. (A) β-Galactosidase activity assays for promoters of the *Bd*AU0158 *bcp-1*, *bcp-2*, and *bcp-3* loci. A *Bd*AU0158 strain harboring a constitutively expressed *lacZ* reporter (P_{S12}-*lacZ*) served as a positive control, whereas a *Bd*AU0158 strain harboring a *lacZ* reporter without a promoter (promoterless) served as a negative control. (B) Competition assays between *Bd*AU0158 *bcp-3*^{C} inhibitor cells and Δ*bcp-3*, Δ*bcp-3 att*Tn*7*::*bcpI-3*, and WT target cells. The dotted line ($\log_{10}$ C.I. = 0) indicates no competitive advantage for inhibitor or target strain. The red-filled circle indicates a competition from which no target cells were recovered following 48 h of coculture. (C) β-Galactosidase activity assays for the *Bd*AU0158 P_{bcp-3} reporter strain cocultured with *Bd*AU0158 *bcp-3*^{C} (*bcp-3*^{C} versus P_{bcp-3}-*lacZ*), as well as the *Bd*AU0158 P_{bcpI-3} reporter strain (P_{bcpI-3}-*lacZ*), with P_{S12}-*lacZ* and promoterless positive and negative controls, respectively, as described for panel A. β-Galactosidase activity assays in panels A and C show results from two biological replicates, each with three technical replicates. ***, $P < 0.001$; ****, $P < 0.0001$, unpaired *t* test. Competition assays in in panel B show results from three biological replicates, each with three technical replicates. Solid horizontal lines represent mean $\log_{10}$ C.I. values. ****, $P < 0.0001$, Mann-Whitney test.

bcp-1, *bcp-2*, and *bcp-3* loci, promoter-*lacZ* fusions (P_{bcp-1}-*lacZ*, P_{bcp-2}-*lacZ*, and P_{bcp-3}-*lacZ*) were constructed and delivered to the *att*Tn*7* site of *Bd*AU0158. Reporter strains were grown in monoculture under the same conditions as those used for competition experiments (LSLB agar at 37°C for 48 h), and β-galactosidase activity was measured. Consistent with results from the competition experiments, the *bcp-1* and *bcp-2* promoters were active under these conditions (Fig. 3A). P_{bcp-1} was more active than P_{bcp-2}, which suggests that the *bcp-1* locus is expressed to a higher degree than the *bcp-2* locus, which may explain why Bcp-1-mediated CDI is more potent than Bcp-2-mediated CDI (Fig. 2A and B). β-Galactosidase activity assays showed that P_{bcp-3} is not active under the conditions used for competitions (Fig. 3A), providing an explanation for why WT *Bd*AU0158 did not outcompete the Δ*bcp-3* mutant.

The *Bd*AU0158 *bcp-3* locus encodes a functional CDI system. To determine if the *Bd*AU0158 *bcp-3* locus encodes a functional CDI system, a strain constitutively expressing the locus (*bcp-3*^{C}) was generated by replacing the native *bcp-3* promoter region with the P_{S12} constitutive promoter. *Bd*AU0158 *bcp-3*^{C} outcompeted the Δ*bcp-3* mutant by 5 log (Fig. 3B), with one competition resulting in no Δ*bcp-3* cells being recovered

from the coculture (red-filled circle in Fig. 3B). The *Bd*AU0158 Δ*bcp-3* mutant was protected from killing by *Bd*AU0158 *bcp-3*^{C} when *bcpI-3* was supplied in *trans*. Surprisingly, WT *Bd*AU0158 cells were not outcompeted by *Bd*AU0158 *bcp-3*^{C}, even though the native P_{bcp-3} appears to be inactive under these conditions (Fig. 3A and B). We hypothesized three scenarios to explain this result: (i) low-level expression of the *bcp-3* locus occurs and cannot be detected by promoter activity assays but leads to sufficient BcpI-3 production to resist Bcp-3-mediated CDI, (ii) CDI attack induces *bcp-3* expression in target cells, or (iii) an internal promoter in the *bcp-3* locus that separately drives expression of *bcpI-3* exists.

An internal promoter in the *Bd*AU0158 *bcp-3* locus separately drives expression of *bcpI-3*. To investigate the possibility that CDI induces *bcp-3* expression in target cells, the *Bd*AU0158 P_{bcp-3}-*lacZ* reporter strain was mixed at a 1:1 ratio with the *Bd*AU0158 *bcp-3*^{C} inhibitor strain (which produces all three CDI systems), and this coculture was incubated at 37°C for 48 h on LSLB agar. The P_{bcp-3}-*lacZ* reporter strain is not susceptible to killing via CDI, as it contains the *bcpI* genes of all three *bcp* loci. β-Galactosidase activity in the *Bd*AU0158 P_{bcp-3}-*lacZ* reporter strain was no greater after coculture with the *Bd*AU0158 *bcp-3*^{C} inhibitor strain than after monoculture (Fig. 3A and C). These results indicate that CDI attack (Bcp-1-, Bcp-2-, or Bcp-3-mediated) does not induce *bcp-3* expression in a target cell.

To determine if an internal promoter resides in the *Bd*AU0158 *bcp-3* locus that drives expression of *bcpI-3*, the last 500 bp of *bcpA-3* (the sequence immediately upstream of and including the *bcpI-3* start codon) was cloned into the *lacZ* expression cassette and the cassette was delivered to the *Bd*AU0158 chromosome, generating the reporter strain *Bd*AU0158 *att*Tn*7*::P_{bcpI-3}-*lacZ*. This strain produced ~1,500 units of β-galactosidase activity after 48 h growth at 37°C on LSLB agar (Fig. 3C), indicating that a promoter (P_{bcpI-3}) resides at the 3′ end of the *Bd*AU0158 *bcpA-3* gene that appears to drive expression of *bcpI-3*, allowing for production of the BcpI-3 antitoxin even when the remainder of the *bcp-3* locus is not expressed.

CDI attack and resistance to CDI do not require the *Bd*AU0158 BcpO proteins. A characteristic of *Burkholderia*-type CDI system-encoding loci is the presence of a fourth ORF, *bcpO*. The function(s) of BcpO proteins has not been determined, although a *Bt*E264 Δ*bcpO* mutant is partially defective at outcompeting *Bt*E264 Δ*bcpAIOB* via CDI (17), indicating that the *Bt*E264 BcpO protein is important for CDI but is not required for this activity. The BcpO protein predicted to be encoded by the *Bd*AU0158 *bcp-1* locus (BcpO-1) shares 90.4% identity at the amino acid level with *Bt*E264 BcpO. There are two and three predicted ORFs between *bcpI* and *bcpB* in the *Bd*AU0158 *bcp-2* and *bcp-3* loci, respectively (Fig. 1A).

Strains containing unmarked, in-frame deletion mutations in each of the BcpO-encoding regions of *Bd*AU0158 were generated, resulting in Δ*bcpO-1*, Δ*bcpO-2*, and Δ*bcpO-3* mutants (deletion schematics shown in Fig. 4). These mutants were competed on LSLB agar for 48 h at 37°C against their parental, *bcp*-intact strains or their respective locus deletion mutants to determine if the *Bd*AU0158 BcpO proteins are required for resistance to CDI or for the ability to kill target cells via CDI, respectively. In accordance with the effect of BcpO on *Bt*E264 CDI (17), the *Bd*AU0158 Δ*bcpO-1* mutant had approximately a 1-log defect in CDI-mediated killing of the *Bd*AU0158 Δ*bcp-1* target strain compared to WT. However, BcpO-1 was not required for resistance to Bcp-1-mediated killing, as the Δ*bcpO-1* mutant was not outcompeted by WT *Bd*AU0158 (Fig. 4A). BcpO-2 was not important for CDI in *Bd*AU0158, as the Δ*bcpO-2* mutant outcompeted the Δ*bcp-2* mutant as well as WT outcompeted Δ*bcp-2*, and the inability of WT to outcompete the Δ*bcpO-2* mutant shows that BcpO-2 was not required for resistance to Bcp-2-mediated CDI (Fig. 4B). Competitions investigating the role of BcpO-3 had to be conducted in the *bcp-3*^{C} background to ensure these genes were expressed. As shown in Fig. 4C, *Bd*AU0158 *bcp-3*^{C} and the *bcp-3*^{C} strain lacking *bcpO-3* (*bcp-3*^{C}Δ*bcpO-3*) were equally able to outcompete Δ*bcp-3* targets, indicating that BcpO-3 was not required for Bcp-3-mediated CDI. Given that target cells with the native *bcp-3* locus promoter are not outcompeted by the constitutively expressing strain (Fig. 3B), a

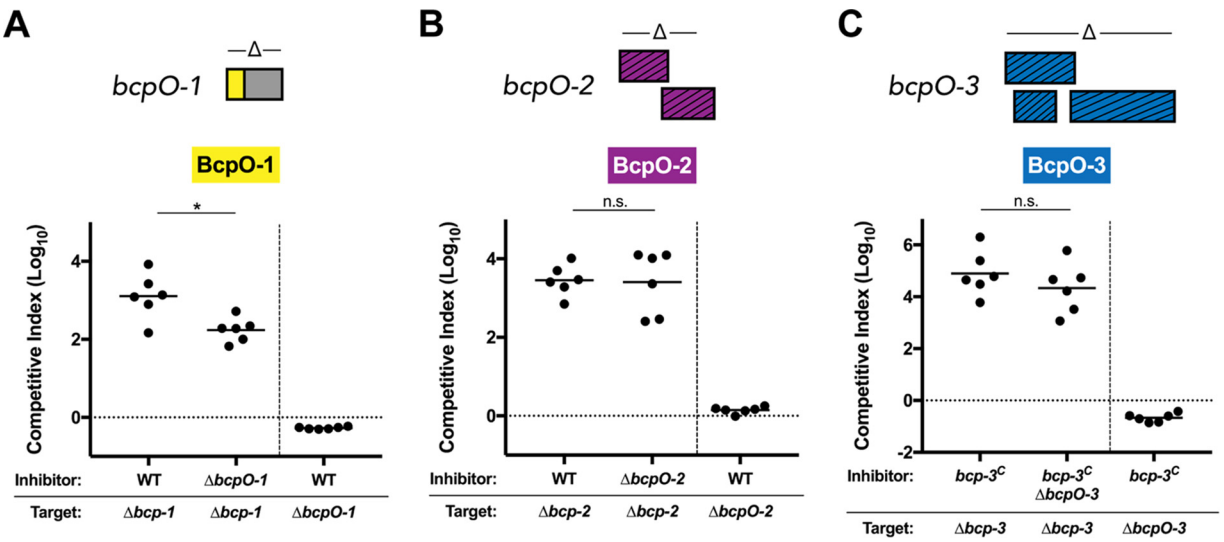

FIG 4 *Bd*AU0158 BcpO proteins are not required for CDI-mediated competition or resistance to CDI. (A) Competition assays between *Bd*AU0158 WT inhibitor cells and Δ*bcp-1* target cells, *Bd*AU0158 Δ*bcpO-1* inhibitor cells and Δ*bcp-1* target cells, and *Bd*AU0158 WT inhibitor cells and Δ*bcpO-1* target cells (right of dashed vertical line). (B) Competition assays between *Bd*AU0158 WT inhibitor cells and Δ*bcp-2* target cells, *Bd*AU0158 Δ*bcpO-2* inhibitor cells and Δ*bcp-2* target cells, and *Bd*AU0158 WT inhibitor cells and Δ*bcpO-2* target cells (right of dashed vertical line). (C) Competition assays between *Bd*AU0158 *bcp-3*^{C} inhibitor cells and Δ*bcp-3* target cells, *Bd*AU0158 *bcp-3*^{C}Δ*bcpO-3* inhibitor cells and Δ*bcp-3* target cells, and *Bd*AU0158 *bcp-3*^{C} inhibitor cells and Δ*bcpO-3* target cells (right of dashed vertical line). *bcpO* gene deletion schematics are shown above each graph. For each competition, results from two separate biological replicates, each with three technical replicates. Solid horizontal lines represent mean $\log_{10}$ C.I. values. Dotted horizontal lines ($\log_{10}$ C.I. = 0) indicate no competitive advantage for inhibitor or target strain. *, $P < 0.05$; n.s., not significant (Mann-Whitney test).

Δ*bcpO-3* mutant in the WT background was used to determine if BcpO-3 is required for resistance to CDI. In agreement with results from competitions investigating BcpO-1 and BcpO-2, the *Bd*AU0158 Δ*bcpO-3* mutant was not susceptible to CDI by a *Bd*AU0158 *bcp-3*^{C} inhibitor (Fig. 4C). In fact, the Δ*bcpO-3* mutant had a slight growth advantage compared to the inhibitor (similar to the Δ*bcp-3 att*Tn*7*::*bcpI-3* and WT targets in Fig. 3B), possibly due to the energetic cost of constitutively producing the Bcp-3 proteins in the *bcp-3*^{C} strain. Together, these data suggest that the BcpO proteins of *Bd*AU0158 do not play a crucial role in CDI.

***Bd*AU0158 does not exhibit Bcp-dependent community behaviors.** Given that *Bd*AU0158 produces three CDI systems, one of which is identical to the *Bt*E264 CDI system, we hypothesized that *Bd*AU0158 could exhibit Bcp-dependent cooperative behaviors (i.e., contact-dependent signaling [CDS]) similar to those seen in *Bt*E264 and that these behaviors may promote infection of the CF respiratory tract. We investigated autoaggregation and pigment production by WT *Bd*AU0158, a panel of mutants that lack one CDI system (Δ*bcp-1*, Δ*bcp-2*, or Δ*bcp-3* mutants) or all three CDI systems (labeled as AU0158 ΔΔΔ), and the strain constitutively expressing the *bcp-3* locus (*bcp-3*^{C}). Autoaggregation of liquid cultures that were grown rotating for 24 h at 37°C in minimal medium was assessed by measuring the optical density at 600 nm (OD_{600}) of a culture after sitting stationary at 25°C for ~30 min and the OD_{600} of the same culture following vigorous vortexing. A vortexed-to-settled OD_{600} ratio greater than 1 indicates that autoaggregation of cells occurred during liquid growth (as seen with WT *Bt*E264 in Fig. 5A), whereas a vortexed/settled OD_{600} ratio of ~1 indicates that cells did not autoaggregate (as seen with *Bt*E264 Δ*bcpAIOB* in Fig. 5A). All *Bd*AU0158 strains had vortexed/settled OD_{600} ratios of ~1, suggesting that *Bd*AU0158 does not autoaggregate under these conditions and that the production of CDI systems, or lack thereof, does not influence this phenotype. Pigment production was assessed by determining the growth of *Bd*AU0158 cells on LSLB agar for 48 h at 37°C and subsequent incubation at 25°C for up to 14 days. Under these conditions, WT *Bt*E264 produced a dark beige pigment, whereas the *Bt*E264 Δ*bcpAIOB* mutant remained white (Fig. 5B). WT *Bd*AU0158 colony biofilms appeared darker than those of the *Bt*E264 Δ*bcpAIOB* mutant, though

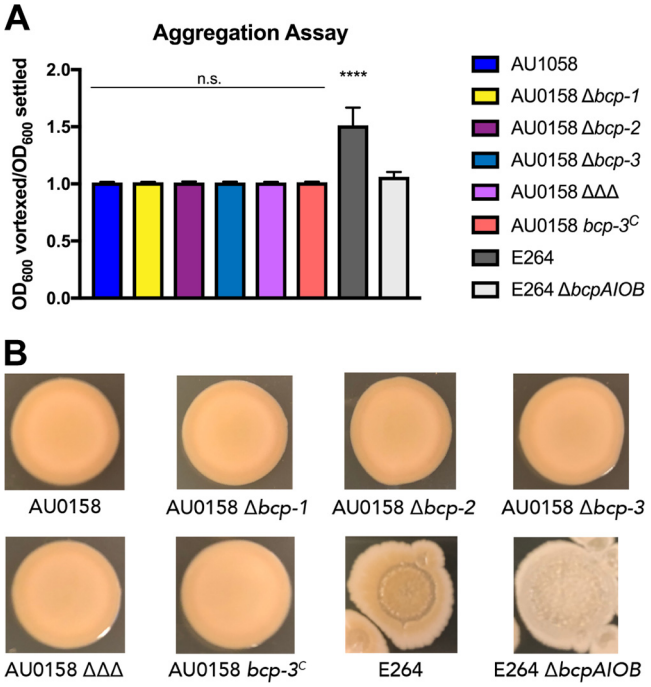

FIG 5 The Bcp-dependent community behaviors of autoaggregation and pigment production are not evident in *Bd*AU0158. (A) Autoaggregation assays of *Bd*AU0158 and *Bt*E264 cultures grown in minimal medium, measured by determining the ratio of OD_{600} values of vortexed and settled cultures. Only *Bt*E264 WT cells exhibit autoaggregation. Results from three separate biological replicates, with mean ratios plotted. Mean ratios compared to nonautoaggregating *Bt*E264 Δ*bcpAIOB* to determine if cells autoaggregated. ****, $P < 0.0001$, Student's *t* test. n.s., not significant. (B) Pigment production assays of *Bd*AU0158 and *Bt*E264 colony biofilms grown on LSLB agar. Only *Bt*E264 exhibits Bcp-dependent pigment production. Images are representative of at least three biological replicates.

this coloration was not dependent on the Bcp proteins, as mutants lacking *bcp* loci and the *bcp-3*^{C} strain appeared similar in color to WT *Bd*AU0158 (Fig. 5B). These results indicate that *Bd*AU0158 does not perform Bcp-dependent cooperative behaviors similar to those seen in *Bt*E264; however, it is possible that the *Bd*AU0158 Bcp proteins do mediate community-based phenotypes and that the assays used to detect *Bt*E264 CDS and its associated phenotypes cannot detect such behaviors in *Bd*AU0158.

Toxicity of *Bd*AU0158 CDI toxins in *E. coli*. To determine if the *Bd*AU0158 BcpA-1-CT, BcpA-2-CT, and BcpA-3-CT are sufficient for toxicity, inducible expression plasmids were generated as derivatives of pET-28(a). Each plasmid contained nucleotide sequences encoding one BcpA-CT [the NX(E/Q)LYN motif through the BcpA stop codon], a CT plus its cognate BcpI [the NX(E/Q)LYN motif through the BcpI stop codon], or one BcpI alone. *Escherichia coli* BL21(DE3) cells harboring these plasmids were grown in LSLB broth, and expression was either induced with isopropyl-β-D-1-thiogalactopyranoside (IPTG) or repressed by D-glucose. Over the time course, OD_{600} was measured and aliquots were plated on solid medium to assess cell viability. To our surprise, production of the *Bd*AU0158 BcpA-1-CT was not toxic in *E. coli*, but production of BcpI-1 was slightly toxic (Fig. 6B). We detected production of both the BcpA-1-CT and BcpI-1 by *E. coli* using sodium dodecyl sulfate-polyacrylamide gel electrophoresis (SDS-PAGE) (see Fig. S1 in the supplemental material). Although induction of *bcp-1* did not cause a decrease in OD_{600} (Fig. 6A), indicating cells were not lysing, the viability of BcpI-1-producing cells over time decreased compared to cells producing either BcpA-1-CT or BcpA-1-CT and BcpI-1 concurrently (Fig. 6B). Cells producing BcpA-1-CT and BcpI-1 concurrently were protected from the toxic effects of BcpI-1, suggesting that binding of the CT to BcpI-1 inhibits toxicity of the immunity protein. We hypothesize that the portion of *Bd*AU0158 BcpA-1-CT being produced in *E. coli* is either larger or smaller than the true toxic protein and that improper folding or processing of the CT

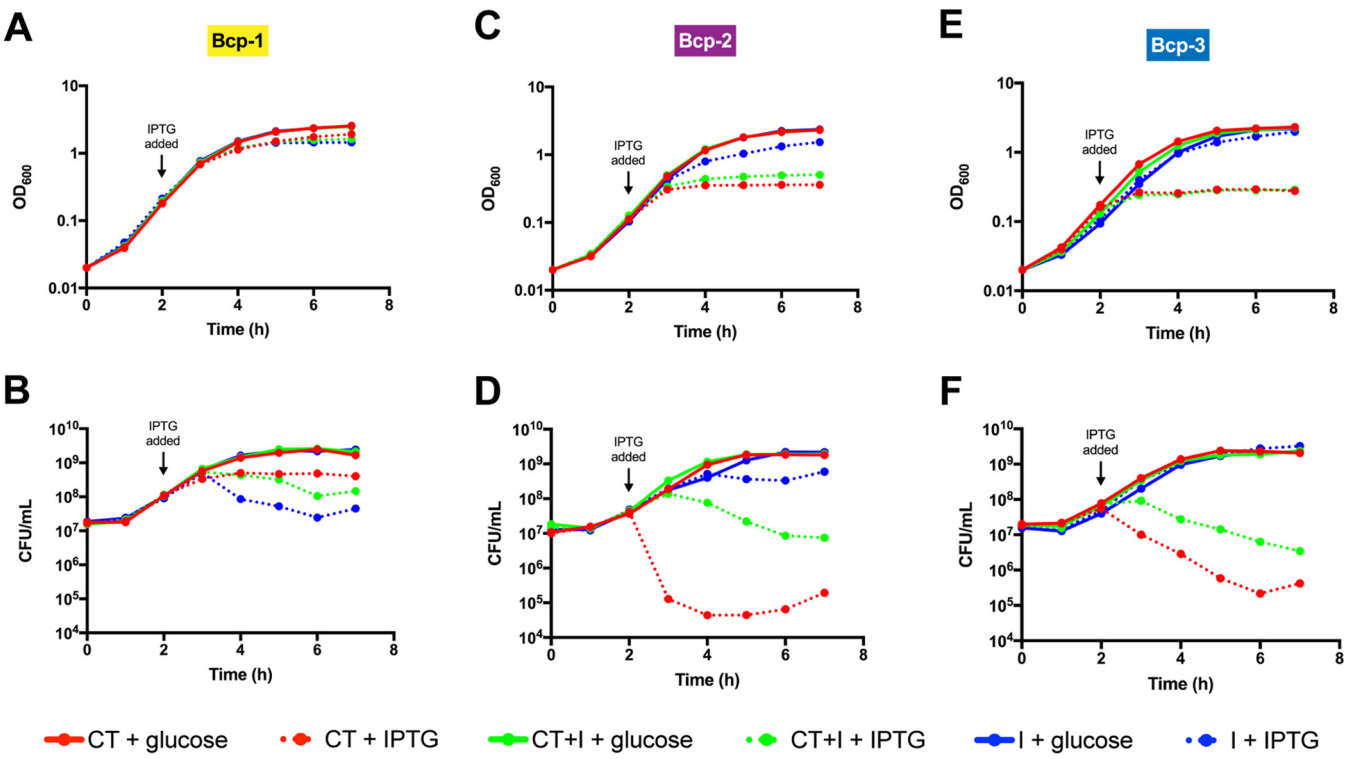

FIG 6 *E. coli* autotoxicity due to inducible production of the *Bd*AU0158 Bcp-2 and Bcp-3 CT toxins but not the Bcp-1 CT toxin. (A, C, E) OD_{600} values of cultures of *E. coli* BL21(DE3) strains producing *Bd*AU0158 Bcp CT toxins (red dotted lines), coproducing CT toxins and BcpI proteins (green dotted lines), and producing BcpI proteins (blue dotted lines) of the Bcp-1 (A), Bcp-2 (C), and Bcp-3 (E) CDI systems. (B, D, F) Cell viability, as measured in CFU per milliliter, of the Bcp-1 protein-producing (B), Bcp-2 protein-producing (D), and Bcp-3 protein-producing (F) *E. coli* BL21(DE3) cultures. Solid lines represent cultures in which *Bd*AU0158 Bcp protein production was repressed by the addition of 0.2% glucose. For each intracellular toxicity assay, means from three biological replicates are plotted.

inhibits its toxic effects. The fact that BcpI-1 is toxic in *E. coli* is more perplexing, as it is not toxic when produced in *Bd*AU0158 (Fig. 2A). Phyre2 analysis (29) predicts that BcpI-1 contains a DNA-binding domain. One possibility is that when BcpI-1 is produced in excess without its cognate BcpA-1-CT, it has deleterious effects in *E. coli* via interactions with genomic DNA.

Unlike *Bd*AU0158 BcpA-1-CT, BcpA-2-CT and BcpA-3-CT were toxic when produced in *E. coli* (Fig. 6D and F). Production of BcpA-2-CT caused the OD_{600} to plateau (Fig. 6C) and resulted in a 4-log decrease in cell viability (Fig. 6D). BcpA-2-CT-producing cells that concurrently produced BcpI-2 were partially rescued from the toxic effects of the BcpA-2-CT, and production of BcpI-2 alone had no deleterious effects on *E. coli* other than the presumed energetic cost of protein production (Fig. 6D). Similar results were found for *bcp-3*; induction did not cause a decrease in OD_{600} (Fig. 6E), but BcpA-3-CT production caused a drastic decrease in cell viability that was partially rescued by concurrent production of BcpI-3 (Fig. 6F). BcpI-3 appears to protect against the toxic effects of the BcpA-3-CT less well than BcpI-2 protects against the effects of BcpA-2-CT (Fig. 6D versus Fig. 6F), though at least partial protection was detected in each case. In these coproducing strains, the BcpA-CTs and BcpI proteins are presumably produced at 1:1 ratios, which may be the reason complete protection against CT-induced toxicity was not detected. It is possible that stoichiometry needs to favor the immunity proteins in order to fully inhibit autotoxicity—a situation that may occur under normal conditions as BcpA proteins are exported out of the cell or may occur if *bcpI*-specific promoters are widespread throughout *bcpAIOB* loci.

The *Bt*E264 Bcp and *Bd*AU0158 Bcp-1 alleles are functionally redundant. The similarity of the predicted amino acid sequences of *Bt*E264 BcpA and *Bd*AU0158 BcpA-1 (Fig. 1B) suggests they are functionally redundant. Previous work in our laboratory

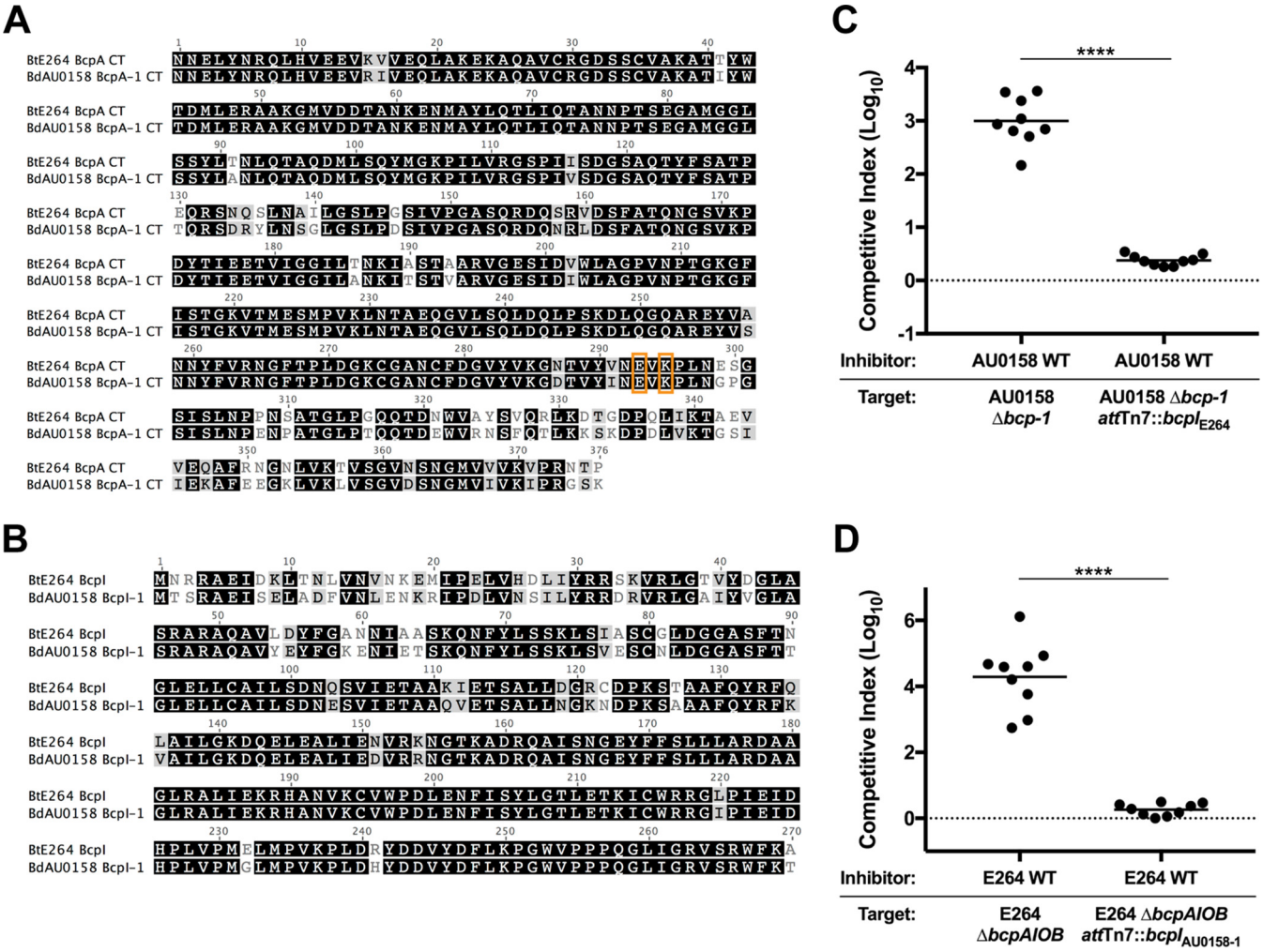

FIG 7 The *Bd*AU0158 Bcp-1 allele contains the same CT toxin-immunity pair as the *Bt*E264 Bcp allele. (A) Amino acid sequence alignment of the *Bd*AU0158 BcpA-1-CT and *Bt*E264 BcpA-CT. The glutamate and lysine residues required for toxicity are boxed in orange. (B) Amino acid sequence alignment of the *Bd*AU0158 BcpI-1 and *Bt*E264 BcpI proteins. For panels A and B, identical residues are highlighted in black, similar residues are highlighted in gray, and disparate residues are not highlighted. (C) Competition assays between *Bd*AU0158 WT inhibitor cells and Δ*bcp-1* and Δ*bcp-1 att*Tn*7*::*bcpI*$_{E264}$ target cells. (D) Competition assays between *Bt*E264 WT inhibitor cells and Δ*bcpAIOB* and Δ*bcpAIOB att*Tn*7*::*bcpI*$_{AU0158-1}$ target cells. For each competition, results are from three separate biological replicates, each with three technical replicates. Solid horizontal lines represent mean $\log_{10}$ C.I. values. Dotted lines ($\log_{10}$ C.I. = 0) indicate no competitive advantage for inhibitor or target strain. ****, $P < 0.0001$, Mann-Whitney test.

identified residues required for the catalytic activity of *Bt*E264 BcpA-CT (E3064 and K3066), and substituting alanines for these residues abrogated CDI activity (20). Glutamate and lysine residues are found at the same positions in *Bd*AU0158 BcpA-1-CT (Fig. 7A). In addition to the similarities of *Bt*E264 BcpA-CT and *Bd*AU0158 BcpA-1-CT, *Bt*E264 BcpI and *Bd*AU0158 BcpI-1 are nearly identical (Fig. 7B). To investigate functional interchangeability, *Bt*E264 Δ*bcpAIOB* and *Bd*AU0158 Δ*bcp-1* mutants were provided with the heterologous *bcpI* gene delivered to the *att*Tn*7* site, generating *Bd*AU0158 Δ*bcp-1 att*Tn*7*::*bcpI*$_{E264}$ and *Bt*E264 Δ*bcpAIOB att*Tn*7*::*bcpI*$_{AU0158-1}$. During 48 h of coculture on LSLB agar at 37°C, the *Bd*AU0158 Δ*bcp-1* mutant was rescued from Bcp-1-mediated CDI by the *Bd*AU0158 WT inhibitor when it constitutively expressed the *Bt*E264 *bcpI* gene ($\log_{10}$ C.I. $\approx$ 0) (Fig. 7C). Similarly, during 24 h of coculture on LSLB agar at 25°C, the *Bt*E264 Δ*bcpAIOB* mutant was rescued from Bcp-mediated CDI by the *Bt*E264 WT inhibitor when it constitutively expressed the *Bd*AU0158 *bcpI-1* gene ($\log_{10}$ C.I. $\approx$ 0) (Fig. 7D). The ability of each BcpI protein to protect against CDI in the heterologous species provides experimental evidence that *Bd*AU0158 and *Bt*E264 share the same CDI system-encoding allele.

DISCUSSION

CDI systems are present in a broad range of Gram-negative bacteria, including many that are pathogenic for animals or plants. Most studies of CDI function have used *Escherichia coli* strain EC93 as a model for *E. coli*-type systems or *Burkholderia thailandensis* strain E264 (*Bt*E264) as a model for *Burkholderia*-type systems (15–17, 19, 22, 23, 31–39). Some experiments have used *E. coli* or *B. thailandensis* strains producing chimeric CdiA or BcpA proteins with toxin domains (and cognate immunity proteins) from pathogens (16, 19, 22, 23, 40), with a smaller number of studies, limited to *E. coli*-type systems, investigating CDI in the pathogen itself (35, 41, 42). In this work, we used the epidemic Bcc isolate *B. dolosa* strain AU0158 (*Bd*AU0158) and showed that its three distinct CDI systems, including two class II *Burkholderia*-type systems, are capable of killing and/or arresting the growth of neighboring bacteria. A whole-genome sequence exists for two additional *B. dolosa* strains, PC543 and LO6 (also referred to as *B. cepacia* strain LO6). The genomes of these strains contain three *bcpAIOB* loci, and the potential proteins encoded by these loci are 100% identical at the amino acid level to the Bcp-1, Bcp-2, and Bcp-3 proteins of *Bd*AU0158, suggesting that CDI by *B. dolosa* is not limited to strain *Bd*AU0158.

While the *Bd*AU0158 Bcp-1 and Bcp-2 CDI systems mediated interbacterial competition under laboratory conditions, Bcp-3-mediated CDI was detected only when the region 5′ to the start of *bcpA-3* was replaced with the constitutively active S12 promoter. These results are consistent with our *lacZ* reporter fusion analyses. The 500-bp and 300-bp DNA fragments corresponding to the regions immediately 5′ to *bcpA-1* and *bcpA-2*, respectively, resulted in substantial β-galactosidase activity when present upstream of *lacZ*, while the corresponding fragment from *bcp-3* resulted in no detectable β-galactosidase activity under the same laboratory conditions. Together with the fact that the gene 5′ to *bcpA-3* is oriented in the opposite direction, the most likely explanation for the results that we obtained for *bcp-3* is that the 500-bp fragment does contain the promoter for *bcp-3* but that this promoter is regulated such that it is not activated under standard laboratory conditions. Little is known about the regulation of any CDI system-encoding genes. In *E. coli*-type systems, the *cdiBAI* genes are expressed under laboratory conditions only in strain EC93 (15, 16, 41), and in *B. thailandensis* E264, the *bcpAIOB* genes appear to be tightly regulated such that only about 1 in 1,000 bacteria express the genes at a high level under laboratory conditions (17). Future experiments will be aimed at identifying transcription start sites and investigating how and why the *bcp* loci are differentially regulated in *Bd*AU0158.

Because the *bcp-3* locus appears to be transcriptionally silent under standard laboratory growth conditions, we were surprised to find that WT *Bd*AU0158 was not outcompeted by the strain expressing *bcp-3* constitutively (*Bd*AU0158 *bcp-3*^{C}). This result led us to search for a promoter for *bcpI-3* within the 3′ end of *bcpA-3*. Although the transcription start site has yet to be determined, the region immediately 5′ to *bcpI-3* was sufficient to drive *lacZ* expression, suggesting that transcription initiation in this region in the native locus results in sufficient BcpI protein production to confer protection from BcpA-3-mediated toxicity. While it would seem to be advantageous for bacteria to produce all immunity proteins at a low level constitutively, our study is the first demonstration, to our knowledge, of a promoter for *bcpI* (or *cdiI*) within a *bcpAIOB* (or *cdiBAI*) operon that is independent of that driving transcription of the rest of the operon. For *E. coli*-type CDI systems, "orphan" *cdiA-CT*/*cdiI* modules that encode functional CdiA-CT toxins and CdiI immunity proteins but are located outside *cdiBAI* loci have been identified (31). These orphan modules, which exist in the genomes of several pathogens containing CDI system-encoding genes (31, 43), share similarities with recombination hot spot (*rhs*) loci and can contribute to diversification of the CDI systems in these species via recombination with the *cdiBAI* genes. There is no evidence that promoters exist for these orphan modules or the corresponding orphan *cdiI* genes (31), and orphan *bcpA-CT*/*bcpI* modules have not been detected in *Burkholderia* spp.

The role of the additional ORF between *bcpI* and *bcpB* in *Burkholderia*-type CDI

system-encoding loci (which we named *bcpO*) remains enigmatic. In class I *Burkholderia*-type loci, the *bcpO* genes are highly homologous. They are predicted to encode small lipoproteins that lack localization of lipoproteins (Lol) avoidance signals, suggesting that they localize to the inner leaflet of the outer membrane. The N-terminal halves of the 53-aa mature polypeptides are rich in prolines, and the C-terminal halves are rich in tryptophans. As with *Bt*E264 (17), deletion of *bcpO-1* in *Bd*AU0158 resulted in a modest decrease in CDI activity, but the mechanism underlying this phenotype is unknown. Our investigations into whether BcpO contributes to CDS or cooperative behaviors have yielded inconclusive results so far. The "*bcpO*" genes in class II *Burkholderia*-type loci bear little similarity to each other or to *bcpO* genes in class I alleles and hence should probably be renamed. Deletion of these ORFs in *Bd*AU0158 *bcp-2* and *bcp-3* had no effect on CDI activity under the conditions tested.

Although we did not detect CDS in *Bd*AU0158, the assays used for these experiments were developed to describe CDS in *Bt*E264 (24) and thus may not be specific for Bcp-mediated community behaviors in other strains. Future investigation into CDS by *Bd*AU0158 and other *Burkholderia* spp. containing *bcpAIOB* loci is warranted. Given the growing appreciation for the impact of bacterial cooperation on pathogenesis (44–48), the virulence of diverse Gram-negative bacterial pathogens may be influenced by CDS.

Production of *Bd*AU0158 BcpA-2-CT and BcpA-3-CT by *E. coli* resulted in autotoxicity that was partially ablated by concurrent production of BcpI-2 and BcpI-3, respectively. Conversely, *E. coli* producing BcpA-1-CT did not exhibit reduced viability, despite the likelihood that this polypeptide contains the toxic domain of BcpA-1. For some *E. coli*-type CDI systems, cytoplasmic "permissive factors" are required for activity of a delivered toxin within a target cell (32, 36, 37). A requirement for a toxicity-promoting factor specific to *Burkholderia*, or to *Bd*AU0158, may explain the lack of toxicity of *Bd*AU0158 BcpA-1-CT in *E. coli*. Alternatively, it is possible that the BcpA-1-CT polypeptide that we selected to produce in *E. coli* BL21(DE3) is not the toxic molecule delivered by the *Bd*AU0158 Bcp-1 CDI system. Indeed, the precise BcpA or CdiA polypeptide that is delivered to the cytoplasm of target cells, and whether it is modified in any way, is not known for any CDI system. We are currently conducting experiments to identify the BcpA polypeptides that are delivered during CDI and CDS in *Bt*E264 and other *Burkholderia* strains.

Also unexpected was the finding that production of *Bd*AU0158 BcpI-1 was toxic in *E. coli*. BcpI-1 is not toxic when produced in *Bd*AU0158, and the nearly identical *Bt*E264 BcpI protein is not toxic when produced in *Bt*E264 (17). Phyre2 analysis predicts a DNA-binding domain in BcpI-1. A possible explanation for its toxicity when massively overproduced in *E. coli* is that it interacts with genomic DNA in a way that blocks an essential function, such as replication or transcription of an essential gene(s). Whether BcpI from either *Bd*AU0158 or *Bt*E264 actually binds DNA is unknown but would be consistent with a role for BcpI, in complex with BcpA-CT, in controlling changes in gene expression during CDS (18, 24).

The high degree of similarity between *bcp-1* of *Bd*AU0158 and *bcpAIOB* of *Bt*E264 and the functional redundancy of the BcpA (24) and BcpI proteins (this work) suggest that these genes represent the same allele. Genomic analyses suggest that both *Burkholderia*- and *E. coli*-type CDI system-encoding genes reside on genomic islands that were mobile at some time in the past and perhaps still are (49–53). We identified 11 *Burkholderia* strains potentially harboring the same CDI system as *Bd*AU0158 and *Bt*E264 by searching for orthologs of *Bd*AU0158 BcpA-1-CT and BcpI-1 (Fig. 8). The Mauve software package (54) detected evidence of synteny surrounding the *bcpAIOB* loci between the three *B. dolosa* strains (*Bd*AU0158, *Bd*PC543, and *Bd*LO6) only. Close examination of these orthologous BcpA-CT and BcpI proteins revealed that although they are highly similar across the different strains, variation in the amino acid sequence exists in the C-terminal portion of BcpA-CT (extreme CT, BcpA-ECT) and the N-terminal portion of BcpI (BcpI-NT) (Fig. 8). We separated these strains into three groups—the *Bd*AU0158/*Bt*E264 group, the *Bglu*BGR1 group, and the *Bt*E444 group—based on the degree of variation of the BcpA-ECTs and BcpI-NTs compared to the *Bd*AU0158 BcpA-

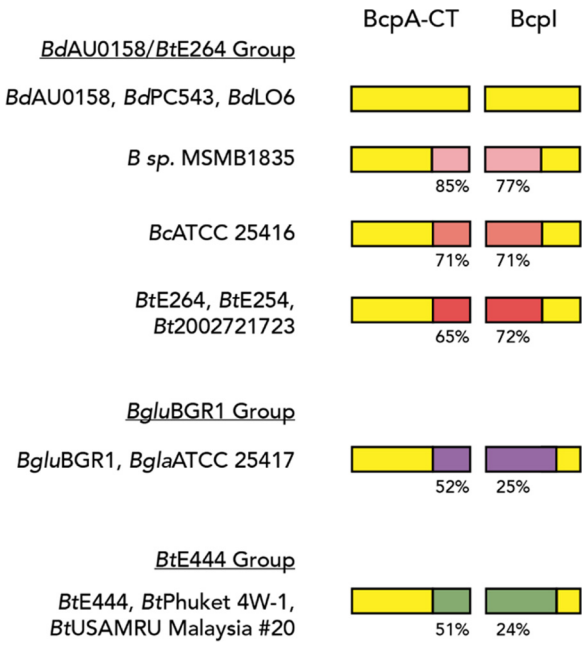

FIG 8 Orthologs of the *Bd*AU0158 BcpA-CT and BcpI across several *Burkholderia* strains. Yellow indicates regions of amino acid sequence identity. Regions of amino acid sequence variation are indicated by shades of pink (*Bd*AU0158/*Bt*E264 group), purple (*Bglu*BGR1 group), and green (*Bt*E444 group), with percent identity to the corresponding *Bd*AU0158 sequence shown below. Members of the *Bd*AU0158/*Bt*E264 group have variable sequences that are more similar to each other than they are to members of the *Bglu*BGR1 and *Bt*E444 groups. *Bd*PC543, *B. dolosa* strain PC543; *Bd*LO6, *B. dolosa* strain LO6 (also called *B. cepacia* LO6); *Bc*ATCC 25416, *B. cepacia* strain ATCC 25416; *Bt*E254, *B. thailandensis* strain E254; *Bt*2002721723, *B. thailandensis* strain 2002721723; *Bglu*BGR1, *B. glumea* strain BGR1; *Bgla*ATCC 25417, *B. gladioli* strain ATCC 25417; *Bt*E444, *B. thailandensis* strain E444; *Bt*Phuket 4W-1, *B. thailandensis* strain Phuket 4W-1; *Bt*USAMRU Malaysia #20, *B. thailandensis* strain USAMRU Malaysia #20; *B.* sp. MSMB1835, species unknown.

ECT and BcpI-NT, respectively. Variation in BcpA-ECT and BcpI-NT sequence, along with the lack of synteny between the regions surrounding *bcpAIOB* in these strains, suggests that if these genes were acquired horizontally, there has been substantial evolution since that time. Though we demonstrated that the BcpA and BcpI proteins of *Bd*AU0158 and *Bt*E264 function in the heterologous species (24; this work), it is unknown whether that holds true for all strains on this list. We hypothesize that the C terminus of BcpI is required for protection against toxicity of the BcpA-CT, given that the BcpI proteins of *Bd*AU0158 and *Bt*E264 block BcpA-CT toxicity in the heterologous species despite exhibiting BcpI-NT sequence variation. Though purely speculative, perhaps these variable regions of BcpA-CT and BcpI are important for CDS and delivery of an "identical" BcpA-CT, from a CDI standpoint, will not elicit CDS in a target cell producing a variable BcpI. Future comparative analyses of these variable alleles will be informative to the mechanisms of both CDI and CDS.

Aside from the investigation of *P. aeruginosa* CDI by Melvin et al. (42), our study is the only demonstration of multiple functional CDI systems in a single pathogenic species. Given the polymicrobial nature of the CF respiratory tract, CDI may provide *Bd*AU0158, as well as *P. aeruginosa*, a competitive advantage during host infection. The genomes of strains of several Bcc species, including *B. cenocepacia*, *B. multivorans*, and *B. vietnamiensis*, contain possible CDI system-encoding genes, and thus these pathogens may benefit from CDI activity during infection. Evolutionary genomic analysis of *B. dolosa* isolates from CF patients over a 16-year period (all originating from the Boston epidemic) revealed that identical nonsynonymous mutations arose in *bcpA-2* across multiple patients, suggesting there is strong selective pressure promoting parallel adaptive evolution of this CDI-encoding gene within the human host (26). Additionally, Bcc species are found ubiquitously in the environment, especially in soil (55), and thus

*Bd*AU0158 could employ its CDI systems to outcompete potential competitors in diverse settings. It is hypothesized that competitive behaviors are the strongest force shaping microbial ecology (5); therefore, *Bd*AU0158 and other Bcp-producing Bcc pathogens may utilize CDI to gain a foothold in the complex polymicrobial environments of the CF respiratory tract and establish long-term, devastating infections in these patients.

MATERIALS AND METHODS

Bacterial strains and growth conditions. All strains used in this study are listed in Table S1 in the supplemental material. *B. dolosa* strains were maintained in either LB (NaCl concentration, 10 g/liter) or low-salt LB (LSLB; NaCl concentration, 5 g/liter), while *B. thailandensis* strains were exclusively maintained in LSLB. Antibiotics were added to select for growth of various *Burkholderia* strains at the following concentrations: 250 μg/ml kanamycin, 50 μg/ml tetracycline, and/or 20 μg/ml chloramphenicol. *E. coli* strains were maintained in LB, and antibiotics were added at the following concentrations when appropriate: 100 μg/ml ampicillin, 50 μg/ml kanamycin, 10 μg/ml tetracycline, and/or 35 μg/ml chloramphenicol. Diaminopimelic acid (DAP) was added at a concentration of 200 μg/ml to cultures maintaining *E. coli* strain RHO3. All strains were grown overnight with aeration at 37°C (unless indicated otherwise).

Construction of plasmids and mutant strains. All plasmids used in this study are listed in Table S2 in the supplemental material and were delivered to *Bd*AU0158 or *Bt*E264 cells via conjugation with *E. coli* RHO3 strains harboring these plasmids. *Bd*AU0158 Δ*bcp-1*, *Bd*AU0158 Δ*bcp-2*, *Bt*E264 Δ*bcpAIOB*, *Bt*E264 *att*Tn*7*::Cm, and *Bt*E264 Δ*bcpAIOB att*Tn*7*::Km were constructed previously (17, 24). Allelic exchange plasmids for generating *Bd*AU0158 in-frame deletion mutants were constructed on the pEXKm5 backbone (56). Briefly, ~500 bp upstream from and including the first three codons of the ORF(s) to be deleted were fused via overlap extension PCR to the last three codons of the ORF(s) and ~500 bp downstream sequence, and constructs were cloned into pEXKm5.

Plasmids to deliver cassettes to the *att*Tn*7* sites of the *Bd*AU0158 and *Bt*E264 chromosomes were constructed using the pUC18Tmini-Tn7T backbone (57). Cassettes for generating antibiotic-resistant *Bd*AU0158 strains were delivered to the *Bd*AU0158 chromosome via triparental mating with *E. coli* RHO3 strains harboring either pUC18T-miniTn7-Km (for kanamycin resistance) or pUC18T-miniTn7-Tet (for tetracycline resistance), as well as the RHO3 strain harboring the transposase-encoding helper plasmid pTNS3 (17). To complement *Bd*AU0158 and *Bt*E264 *bcp* locus deletion mutants with various *bcpI* genes, the genes of interest were cloned into pUCS12Km (pUC18T-miniTn7-Km plasmid with the constitutive *Bt*E264 ribosomal S12 subunit gene promoter cloned immediately 5′ to the multiple cloning site), and these P_{S12}-driven constructs were delivered to a neutral site in the chromosome via triparental mating with *E. coli* RHO3 harboring pTNS3. Plasmids containing *lacZ* reporter cassettes were generated on the pUC*lacZ* backbone (pUC18T-miniTn7-Km with promoterless *lacZ* cloned into the multiple cloning site), with promoters of interest inserted immediately 5′ to the *lacZ* gene. *lacZ* reporter cassettes were delivered to the *Bd*AU0158 chromosome via triparental mating with *E. coli* RHO3 harboring pTNS3.

Interbacterial competition experiments. All competitions between *Bd*AU0158 strains followed our previously developed protocol (17), with minor adjustments. Cells from overnight cultures were washed in phosphate-buffered saline (PBS) and diluted to an OD_{600} value of 0.2. Equal volumes of inhibitor and target cells were mixed, and 20-μl spots of cell suspensions were plated on LSLB agar and allowed to dry. Once spots had dried, competitions were incubated at 37°C for 48 h. To determine the starting ratios for competitions, the cell suspensions containing inhibitor and target bacteria were serially diluted and 20-μl spots were plated onto selective medium (LSLB/Km_{250} or LSLB/Tet_{50}) and incubated at 37°C. Following 48 h of coculture, cells were sampled from the edge of the colony biofilms, resuspended in 1 ml PBS, and serially diluted, and 20-μl spots of serial dilutions were plated onto selective medium (LSLB/Km_{250} or LSLB/Tet_{50}) and incubated at 37°C. Competitions involving *Bt*E264 were conducted similarly, except that cocultures were incubated at room temperature for 24 h. Colony counts for inhibitor and target bacteria at the starting and 24-h or 48-h time points were used to determine the competitive index (C.I.) for each competition experiment, according to the equation C.I. = ($inhibitor_{tx}$/$target_{tx}$)/($inhibitor_{t0}$/$target_{t0}$), with *tx* representing either the 24-h or 48-h time point and *t*0 representing starting time point. A positive $\log_{10}$ C.I. indicates that the inhibitor strain outcompeted the target strain, a negative $\log_{10}$ C.I. indicates that the target strain outcompeted the inhibitor strain, and a $\log_{10}$ C.I. of ~0 indicates no competition in favor of either strain.

***β*-Galactosidase activity assays.** Cells from overnight cultures were washed in PBS and diluted to an OD_{600} value of 0.2. Twenty-microliter spots of cell suspensions were plated on LSLB agar, and after spots had dried, cells were incubated at 37°C for 48 h. For the coculture with *Bd*AU0158 *bcp-3*^{C} and *Bd*AU0158 *att*Tn*7*::$P_{bcp\text{-}3}$-*lacZ*, strains were mixed at a 1:1 ratio, and 20-μl spots were plated onto LSLB and incubated at 37°C for 48 h. Following incubation, entire colony biofilms were resuspended in 1 ml PBS and diluted 1:10 in Z-buffer plus 0.27% β-mercaptoethanol (Fisher Scientific), and 250 μl was removed to measure OD_{600} values. To permeabilize cells, 50 μl chloroform and 10 μl 0.1% sodium dodecyl sulfate were added to the remaining 750-μl cell suspensions and samples were vortexed and allowed to settle. Fifty microliters of permeabilized cells and 50 μl 4-mg/ml *ortho*-nitrophenyl-β-galactoside were added to 150 μl Z-buffer, and OD_{420} values were measured every minute over a 20-min time course. OD_{420} values for two time points within the linear range and the corresponding change in time were used to calculate β-galactoside activity with the following formula: β-galactoside activity = [ΔOD_{420}/($\Delta t \times 0.05$ ml cells $\times$ OD_{600})] $\times$ 1,000.

Z-buffer was prepared (per liter) as follows: 50 mM Na_2HPO_4 (anhydrous), 40 mM NaH_2PO_4, 10 mM KCl, and 1 mM $MgSO_4$ (anhydrous).

Intracellular toxicity assays. *E. coli* BL21(DE3) cells harboring IPTG-inducible plasmids were grown overnight in LB plus kanamycin. Cells were washed in PBS, subcultured in 50 ml LSLB plus kanamycin at a starting OD_{600} of 0.02 (with D-glucose added at a final concentration of 0.2% for noninduced cultures), and grown at 37°C with aeration for 7 h. Samples were taken hourly to determine OD_{600} values of the cultures, as well as to plate serial dilutions on LB agar plus kanamycin supplemented with 0.2% D-glucose to determine cell viability. At the 2-h time point, IPTG was added at a final concentration of 0.5 mM to induce expression of *bcp* constructs. Production of BcpA-1-CT and Bcpl-1 was assessed via separation in a 12% SDS-PAGE gel and Coomassie blue staining.

Aggregation assays. Cells from overnight cultures were washed in PBS and inoculated into 2 ml M63 minimal medium (3 g/liter KH_2PO_4, 7 g/liter K_2HPO_4, 2 g/liter $(NH_4)_2SO_4$, 0.5 g/liter $FeSO_4$, 0.2% glucose, 1 mM $MgSO_4$, 0.4% glycerol, 0.01% Casamino Acids) at a starting OD_{600} of 0.2. Aggregation cultures were grown on a rotator drum at 37°C for 24 h. After 24 h, culture tubes were taken off the rotator drum and incubated statically at 25°C for ~30 min to allow cells to settle, and the OD_{600} values of settled cultures were measured. The tubes were then vigorously vortexed to homogenize the cultures, and the OD_{600} values of vortexed cultures were measured.

Pigment production assays. Cells from overnight cultures were washed twice in PBS and diluted to an OD_{600} value of 0.2, and 20-μl spots were plated onto LSLB agar. After spots had dried, plates were wrapped in paraffin film and incubated at 25°C for 14 days.

Bioinformatic analyses. *Bt*E264 BcpB homologs were identified using the National Center for Biotechnology Information BLASTP suite. *Burkholderia* strains harboring the same BcpA-CT as the allele shared by *Bt*E264 and *Bd*AU0158 were identified using the *Burkholderia* Genome Database (58). ORF predictions were conducted with the Geneious 8 software package (30), and genome comparisons using the Mauve plug-in (54) were conducted on Geneious 8. Protein alignments were conducted using the Clustal Omega online server (59). Protein structure predictions were conducted using the Phyre2 online server (29). Signal sequence identification was performed using the SignalP 4.1 online server (60).

SUPPLEMENTAL MATERIAL

Supplemental material for this article may be found at https://doi.org/10.1128/JB.00428-18.

SUPPLEMENTAL FILE 1, PDF file, 0.3 MB.

ACKNOWLEDGMENTS

We thank members of the Cotter Laboratory for support, thoughtful discussion, and critical reading of the manuscript. We also thank Erin Garcia for insight and technical assistance.

This work was supported by NIH awards NIHR01GM121110 and NIHR21AI112764 to P.A.C. and Cystic Fibrosis Foundation award COTTER1810 to P.A.C.

Funders had no role in the design, execution, or analysis of this study or in the preparation and submission of the manuscript.

REFERENCES

1. Hansen SK, Rainey PB, Haagensen JAJ, Molin S. 2007. Evolution of species interactions in a biofilm community. Nature 445:533–536. https://doi.org/10.1038/nature05514.
2. Ren D, Madsen JS, Sørensen SJ, Burmølle M. 2015. High prevalence of biofilm synergy among bacterial soil isolates in cocultures indicates bacterial interspecific cooperation. ISME J 9:81–89. https://doi.org/10.1038/ismej.2014.96.
3. Rendueles O, Ghigo J-M. 2015. Mechanisms of competition in biofilm communities. Microbiol Spectr 3:319–342. https://doi.org/10.1128/microbiolspec.MB-0009-2014.
4. Flemming H-C, Wingender J, Szewzyk U, Steinberg P, Rice SA, Kjelleberg S. 2016. Biofilms: an emergent form of bacterial life. Nat Rev Microbiol 14:563–575. https://doi.org/10.1038/nrmicro.2016.94.
5. Foster KR, Bell T. 2012. Competition, not cooperation, dominates interactions among culturable microbial species. Curr Biol 22:1845–1850. https://doi.org/10.1016/j.cub.2012.08.005.
6. Sekirov I, Russell SL, Antunes LCM, Finlay BB. 2010. Gut microbiota in health and disease. Physiol Rev 90:859–904. https://doi.org/10.1152/physrev.00045.2009.
7. Ma B, Forney LJ, Ravel J. 2012. Vaginal microbiome: rethinking health and disease. Annu Rev Microbiol 66:371–389. https://doi.org/10.1146/annurev-micro-092611-150157.
8. Filkins LM, O'Toole GA. 2015. Cystic fibrosis lung infections: polymicrobial, complex, and hard to treat. PLoS Pathog 11:e1005258. https://doi.org/10.1371/journal.ppat.1005258.
9. Zhao J, Schloss PD, Kalikin LM, Carmody LA, Foster BK, Petrosino JF, Cavalcoli JD, VanDevanter DR, Murray S, Li JZ, Young VB, Lipuma JJ. 2012. Decade-long bacterial community dynamics in cystic fibrosis airways. Proc Natl Acad Sci U S A 109:5809–5814. https://doi.org/10.1073/pnas.1120577109.
10. Lipuma JJ. 2010. The changing microbial epidemiology in cystic fibrosis. Clin Microbiol Rev 23:299–323. https://doi.org/10.1128/CMR.00068-09.
11. Isles A, Maclusky I, Corey M, Gold R, Prober C, Fleming P, Levison H. 1984. Pseudomonas cepacia infection in cystic fibrosis: an emerging problem. J Pediatr 104:206–210. https://doi.org/10.1016/S0022-3476(84)80993-2.
12. Schwab U, Abdullah LH, Perlmutt OS, Albert D, Davis CW, Arnold RR, Yankaskas JR, Gilligan P, Neubauer H, Randell SH, Boucher RC. 2014. Localization of Burkholderia cepacia complex bacteria in cystic fibrosis lungs and interactions with Pseudomonas aeruginosa in hypoxic mucus. Infect Immun 82:4729–4745. https://doi.org/10.1128/IAI.01876-14.
13. Carmody LA, Zhao J, Kalikin LM, LeBar W, Simon RH, Venkataraman A, Schmidt TM, Abdo Z, Schloss PD, Lipuma JJ. 2015. The daily dynamics of cystic fibrosis airway microbiota during clinical stability and at exacerbation. Microbiome 3:12. https://doi.org/10.1186/s40168-015-0074-9.
14. Bernier SP, Workentine ML, Li X, Magarvey NA, O'Toole GA, Surette MG. 2016. Cyanide toxicity to Burkholderia cenocepacia is modulated by

polymicrobial communities and environmental factors. Front Microbiol 7:725. https://doi.org/10.3389/fmicb.2016.00725.
15. Aoki SK, Pamma R, Hernday AD, Bickham JE, Braaten BA, Low DA. 2005. Contact-dependent inhibition of growth in Escherichia coli. Science 309:1245–1248. https://doi.org/10.1126/science.1115109.
16. Aoki SK, Diner EJ, de Roodenbeke CT, Burgess BR, Poole SJ, Braaten BA, Jones AM, Webb JS, Hayes CS, Cotter PA, Low DA. 2010. A widespread family of polymorphic contact-dependent toxin delivery systems in bacteria. Nature 468:439–442. https://doi.org/10.1038/nature09490.
17. Anderson MS, Garcia EC, Cotter PA. 2012. The Burkholderia bcpAIOB genes define unique classes of two-partner secretion and contact dependent growth inhibition systems. PLoS Genet 8:e1002877. https://doi.org/10.1371/journal.pgen.1002877.
18. Danka ES, Garcia EC, Cotter PA. 2017. Are CDI systems multicolored, facultative, helping greenbeards? Trends Microbiol 25:391–401. https://doi.org/10.1016/j.tim.2017.02.008.
19. Anderson MS, Garcia EC, Cotter PA. 2014. Kind discrimination and competitive exclusion mediated by contact-dependent growth inhibition systems shape biofilm community structure. PLoS Pathog 10:e1004076. https://doi.org/10.1371/journal.ppat.1004076.
20. Garcia EC, Anderson MS, Hagar JA, Cotter PA. 2013. Burkholderia BcpA mediates biofilm formation independently of interbacterial contact-dependent growth inhibition. Mol Microbiol 89:1213–1225. https://doi.org/10.1111/mmi.12339.
21. Garcia EC. 2018. Contact-dependent interbacterial toxins deliver a message. Curr Opin Microbiol 42:40–46. https://doi.org/10.1016/j.mib.2017.09.011.
22. Nikolakakis K, Amber S, Wilbur JS, Diner EJ, Aoki SK, Poole SJ, Tuanyok A, Keim PS, Peacock S, Hayes CS, Low DA. 2012. The toxin/immunity network of Burkholderia pseudomallei contact-dependent growth inhibition (CDI) systems. Mol Microbiol 84:516–529. https://doi.org/10.1111/j.1365-2958.2012.08039.x.
23. Koskiniemi S, Garza-Sánchez F, Edman N, Chaudhuri S, Poole SJ, Manoil C, Hayes CS, Low DA. 2015. Genetic analysis of the CDI pathway from Burkholderia pseudomallei 1026b. PLoS One 10:e0120265. https://doi.org/10.1371/journal.pone.0120265.
24. Garcia EC, Perault AI, Marlatt SA, Cotter PA. 2016. Interbacterial signaling via Burkholderia contact-dependent growth inhibition system proteins. Proc Natl Acad Sci U S A 113:8296–8301. https://doi.org/10.1073/pnas.1606323113.
25. Vermis K, Coenye T, Lipuma JJ, Mahenthiralingam E, Nelis HJ, Vandamme P. 2004. Proposal to accommodate Burkholderia cepacia genomovar VI as Burkholderia dolosa sp. nov. Int J Syst Evol Microbiol 54:689–691. https://doi.org/10.1099/ijs.0.02888-0.
26. Lieberman TD, Michel J-B, Aingaran M, Potter-Bynoe G, Roux D, Davis MR, Skurnik D, Leiby N, Lipuma JJ, Goldberg JB, McAdam AJ, Priebe GP, Kishony R. 2011. Parallel bacterial evolution within multiple patients identifies candidate pathogenicity genes. Nat Genet 43:1275–1280. https://doi.org/10.1038/ng.997.
27. Biddick R, Spilker T, Martin A, Lipuma JJ. 2003. Evidence of transmission of Burkholderia cepacia, Burkholderia multivorans and Burkholderia dolosa among persons with cystic fibrosis. FEMS Microbiol Lett 228:57–62. https://doi.org/10.1016/S0378-1097(03)00724-9.
28. Kalish LA, Waltz DA, Dovey M, Potter-Bynoe G, McAdam AJ, Lipuma JJ, Gerard C, Goldmann D. 2006. Impact of Burkholderia dolosa on lung function and survival in cystic fibrosis. Am J Respir Crit Care Med 173:421–425. https://doi.org/10.1164/rccm.200503-344OC.
29. Kelley LA, Mezulis S, Yates CM, Wass MN, Sternberg MJE. 2015. The Phyre2 web portal for protein modeling, prediction and analysis. Nat Protoc 10:845–858. https://doi.org/10.1038/nprot.2015.053.
30. Kearse M, Moir R, Wilson A, Stones-Havas S, Cheung M, Sturrock S, Buxton S, Cooper A, Markowitz S, Duran C, Thierer T, Ashton B, Meintjes P, Drummond A. 2012. Geneious Basic: an integrated and extendable desktop software platform for the organization and analysis of sequence data. Bioinformatics 28:1647–1649. https://doi.org/10.1093/bioinformatics/bts199.
31. Poole SJ, Diner EJ, Aoki SK, Braaten BA, t' Kint de Roodenbeke C, Low DA, Hayes CS. 2011. Identification of functional toxin/immunity genes linked to contact-dependent growth inhibition (CDI) and rearrangement hotspot (Rhs) systems. PLoS Genet 7:e1002217. https://doi.org/10.1371/journal.pgen.1002217.
32. Diner EJ, Beck CM, Webb JS, Low DA, Hayes CS. 2012. Identification of a target cell permissive factor required for contact-dependent growth inhibition (CDI). Genes Dev 26:515–525. https://doi.org/10.1101/gad.182345.111.
33. Ruhe ZC, Wallace AB, Low DA, Hayes CS. 2013. Receptor polymorphism restricts contact-dependent growth inhibition to members of the same species. mBio 4:e00480-13. https://doi.org/10.1128/mBio.00480-13.
34. Webb JS, Nikolakakis KC, Willett JLE, Aoki SK, Hayes CS, Low DA. 2013. Delivery of CdiA nuclease toxins into target cells during contact-dependent growth inhibition. PLoS One 8:e57609. https://doi.org/10.1371/journal.pone.0057609.
35. Beck CM, Willett JLE, Cunningham DA, Kim JJ, Low DA, Hayes CS. 2016. CdiA effectors from uropathogenic Escherichia coli use heterotrimeric osmoporins as receptors to recognize target bacteria. PLoS Pathog 12:e1005925. https://doi.org/10.1371/journal.ppat.1005925.
36. Johnson PM, Beck CM, Morse RP, Garza-Sánchez F, Low DA, Hayes CS, Goulding CW. 2016. Unraveling the essential role of CysK in CDI toxin activation. Proc Natl Acad Sci U S A 113:9792–9797. https://doi.org/10.1073/pnas.1607112113.
37. Jones AM, Garza-Sánchez F, So J, Hayes CS, Low DA. 2017. Activation of contact-dependent antibacterial tRNase toxins by translation elongation factors. Proc Natl Acad Sci U S A 114:E1951–E1957. https://doi.org/10.1073/pnas.1619273114.
38. Ruhe ZC, Nguyen JY, Xiong J, Koskiniemi S, Beck CM, Perkins BR, Low DA, Hayes CS. 2017. CdiA effectors use modular receptor-binding domains to recognize target bacteria. mBio 8:e00290-17. https://doi.org/10.1128/mBio.00290-17.
39. Ghosh A, Baltekin Ö, Wäneskog M, Elkhalifa D, Hammarlöf DL, Elf J, Koskiniemi S. 2018. Contact-dependent growth inhibition induces high levels of antibiotic-tolerant persister cells in clonal bacterial populations. EMBO J 37:e98026. https://doi.org/10.15252/embj.201798026.
40. Morse RP, Willett JLE, Johnson PM, Zheng J, Credali A, Iniguez A, Nowick JS, Hayes CS, Goulding CW. 2015. Diversification of β-augmentation interactions between CDI toxin/immunity proteins. J Mol Biol 427:3766–3784. https://doi.org/10.1016/j.jmb.2015.09.020.
41. Beck CM, Morse RP, Cunningham DA, Iniguez A, Low DA, Goulding CW, Hayes CS. 2014. CdiA from Enterobacter cloacae delivers a toxic ribosomal RNase into target bacteria. Structure 22:707–718. https://doi.org/10.1016/j.str.2014.02.012.
42. Melvin JA, Gaston JR, Phillips SN, Springer MJ, Marshall CW, Shanks RMQ, Bomberger JM. 2017. Pseudomonas aeruginosa contact-dependent growth inhibition plays dual role in host-pathogen interactions. mSphere 2:e00336-17. https://doi.org/10.1128/mSphere.00336-17.
43. Arenas J, Schipper K, van Ulsen P, van der Ende A, Tommassen J. 2013. Domain exchange at the 3′ end of the gene encoding the fratricide meningococcal two-partner secretion protein A. BMC Genomics 14:622. https://doi.org/10.1186/1471-2164-14-622.
44. Griffin AS, West SA, Buckling A. 2004. Cooperation and competition in pathogenic bacteria. Nature 430:1024–1027. https://doi.org/10.1038/nature02744.
45. Rumbaugh KP, Diggle SP, Watters CM, Ross-Gillespie A, Griffin AS, West SA. 2009. Quorum sensing and the social evolution of bacterial virulence. Curr Biol 19:341–345. https://doi.org/10.1016/j.cub.2009.01.050.
46. Raymond B, West SA, Griffin AS, Bonsall MB. 2012. The dynamics of cooperative bacterial virulence in the field. Science 337:85–88. https://doi.org/10.1126/science.1218196.
47. Stacy A, McNally L, Darch SE, Brown SP, Whiteley M. 2016. The biogeography of polymicrobial infection. Nat Rev Microbiol 14:93–105. https://doi.org/10.1038/nrmicro.2015.8.
48. Nadell CD, Drescher K, Foster KR. 2016. Spatial structure, cooperation and competition in biofilms. Nat Rev Microbiol 14:589–600. https://doi.org/10.1038/nrmicro.2016.84.
49. Holden MTG, Titball RW, Peacock SJ, Cerdeño-Tárraga AM, Atkins T, Crossman LC, Pitt T, Churcher C, Mungall K, Bentley SD, Sebaihia M, Thomson NR, Bason N, Beacham IR, Brooks K, Brown KA, Brown NF, Challis GL, Cherevach I, Chillingworth T, Cronin A, Crossett B, Davis P, DeShazer D, Feltwell T, Fraser A, Hance Z, Hauser H, Holroyd S, Jagels K, Keith KE, Maddison M, Moule S, Price C, Quail MA, Rabbinowitsch E, Rutherford K, Sanders M, Simmonds M, Songsivilai S, Stevens K, Tumapa S, Vesaratchavest M, Whitehead S, Yeats C, Barrell BG, Oyston PCF, Parkhill J. 2004. Genomic plasticity of the causative agent of melioidosis, Burkholderia pseudomallei. Proc Natl Acad Sci U S A 101:14240–14245. https://doi.org/10.1073/pnas.0403302101.
50. Yu Y, Kim HS, Chua HH, Lin CH, Sim SH, Lin D, Derr A, Engels R, DeShazer D, Birren B, Nierman WC, Tan P. 2006. Genomic patterns of pathogen evolution revealed by comparison of Burkholderia pseudomallei, the causative agent of melioidosis, to avirulent Burkholderia thailandensis. BMC Microbiol 6:46. https://doi.org/10.1186/1471-2180-6-46.

51. Tuanyok A, Auerbach RK, Brettin TS, Bruce DC, Munk AC, Detter JC, Pearson T, Hornstra H, Sermswan RW, Wuthiekanun V, Peacock SJ, Currie BJ, Keim P, Wagner DM. 2007. A horizontal gene transfer event defines two distinct groups within Burkholderia pseudomallei that have dissimilar geographic distributions. J Bacteriol 189:9044–9049. https://doi.org/10.1128/JB.01264-07.
52. Tuanyok A, Leadem BR, Auerbach RK, Beckstrom-Sternberg SM, Beckstrom-Sternberg JS, Mayo M, Wuthiekanun V, Brettin TS, Nierman WC, Peacock SJ, Currie BJ, Wagner DM, Keim P. 2008. Genomic islands from five strains of Burkholderia pseudomallei. BMC Genomics 9:566. https://doi.org/10.1186/1471-2164-9-566.
53. Ruhe ZC, Nguyen JY, Chen AJ, Leung NY, Hayes CS, Low DA. 2016. CDI systems are stably maintained by a cell-contact mediated surveillance mechanism. PLoS Genet 12:e1006145. https://doi.org/10.1371/journal.pgen.1006145.
54. Darling ACE, Mau B, Blattner FR, Perna NT. 2004. Mauve: multiple alignment of conserved genomic sequence with rearrangements. Genome Res 14:1394–1403. https://doi.org/10.1101/gr.2289704.
55. Mahenthiralingam E, Urban TA, Goldberg JB. 2005. The multifarious, multireplicon Burkholderia cepacia complex. Nat Rev Microbiol 3:144–156. https://doi.org/10.1038/nrmicro1085.
56. López CM, Rholl DA, Trunck LA, Schweizer HP. 2009. Versatile dual-technology system for markerless allele replacement in Burkholderia pseudomallei. Appl Environ Microbiol 75:6496–6503. https://doi.org/10.1128/AEM.01669-09.
57. Choi K-H, Gaynor JB, White KG, Lopez C, Bosio CM, Karkhoff-Schweizer RR, Schweizer HP. 2005. A Tn7-based broad-range bacterial cloning and expression system. Nat Methods 2:443–448. https://doi.org/10.1038/nmeth765.
58. Winsor GL, Khaira B, Van Rossum T, Lo R, Whiteside MD, Brinkman FSL. 2008. The Burkholderia Genome Database: facilitating flexible queries and comparative analyses. Bioinformatics 24:2803–2804. https://doi.org/10.1093/bioinformatics/btn524.
59. Sievers F, Wilm A, Dineen D, Gibson TJ, Karplus K, Li W, Lopez R, McWilliam H, Remmert M, Söding J, Thompson JD, Higgins DG. 2011. Fast, scalable generation of high-quality protein multiple sequence alignments using Clustal Omega. Mol Syst Biol 7:539–539. https://doi.org/10.1038/msb.2011.75.
60. Nielsen H. 2017. Predicting secretory proteins with SignalP. Methods Mol Biol 1611:59–73. https://doi.org/10.1007/978-1-4939-7015-5_6.